

ent techniques will shed light on the influence of microstructural parameters other than grain size, such as twin density and subgrain boundaries. This technique has a clear advantage over in situ tensile deformation in the transmission microscope, because the high energy of the light source guarantees a better statistical approach and excludes thin-film artifacts.

Direct Spinning of Carbon Nanotube Fibers from Chemical Vapor Deposition Synthesis

Ya-Li Li, Ian A. Kinloch, Alan H. Windle*

References and Notes

- H. Mughrabi, in *Plastic Deformation and Fracture of Materials*, R. W. Cahn, P. Haasen, E. J. Kramer, Eds., vol. 6 of *Materials Science and Technology* (Wiley-VCH, Weinheim, Germany, 1991), pp. 1–19.
- M. Legros, B. R. Elliott, M. N. Rittner, J. R. Weertman, K. J. Hemker, *Philos. Mag. A* **80**, 1017 (2000).
- J. R. Weertman, *Mechanical Behaviour of Nanocrystalline Metals in Nanostructured Materials: Processing, Properties, and Potential Applications* (William Andrew, Norwich, NY, 2002).
- K. S. Kumar, S. Suresh, M. F. Chisholm, J. A. Horton, P. Wang, *Acta Mater.* **51**, 387 (2003).
- M. Chen *et al.*, *Science* **300**, 1275 (2003).
- R. C. Hugo *et al.*, *Acta Mater.* **51**, 1937 (2003).
- S. X. McFadden, A. V. Sergueeva, T. Kruml, J.-L. Martin, A. K. Mukherjee, *MRS Symp. Ser.* **634**, B1.3.1 (2001).
- P. M. Derlet, H. Van Swygenhoven, *Philos. Mag. A* **82**, 1 (2002).
- H. Van Swygenhoven, P. M. Derlet, *Phys. Rev. B* **64**, 224105 (2001).
- H. Van Swygenhoven, P. M. Derlet, A. Hasnaoui, *Phys. Rev. B* **66**, 024101 (2002).
- H. Van Swygenhoven, *Science* **296**, 66 (2002).
- V. Yamakov, D. Wolf, S. E. Phillpot, A. K. Mukherjee, H. Gleiter, *Nature Mater.* **1**, 1 (2002).
- P. M. Derlet, A. Hasnaoui, H. Van Swygenhoven, *Scr. Mater.* **49**, 629 (2003).
- H. Van Swygenhoven, P. M. Derlet, Z. Budrovic, A. Hasnaoui, *Z. Metallkd.* **94**, 1106 (2003).
- J. Schiøtz, K. W. Jacobsen, *Science* **301**, 1357 (2003).
- H. P. Klug, L. E. Alexander, *X-ray Diffraction Procedures for Polycrystalline and Amorphous Materials* (Wiley, New York, ed. 2, 1974).
- K. Reimann, R. Würschum, *J. Appl. Phys.* **81**, 7186 (1997).
- T. Ungar, J. Gubicza, G. Ribarik, A. Borbely, *J. Appl. Crystallogr.* **34**, 298 (2001).
- Information about the SLS and the microstrip detector can be found at <http://sls.web.psi.ch>.
- F. Dalla Torre, H. Van Swygenhoven, M. Victoria, *Acta Mater.* **50**, 3957 (2002).
- Z. Budrovic, H. Van Swygenhoven, P. M. Derlet, S. Van Petegem, B. Schmitt, data not shown.
- See supporting data on Science Online.
- Y. Champion *et al.*, *Science* **300**, 310 (2003).
- D. Jia *et al.*, *Appl. Phys. Lett.* **79**, 611 (2001).
- Y. M. Wang, E. Ma, *Acta Mater.* **52**, 1699 (2004).
- B. E. Warren, *X-ray Diffraction* (Addison-Wesley, Reading, MA, 1969).
- M. A. Krivoglaz, *X-ray and Neutron Diffraction in Nonideal Crystals* (Springer, Berlin, 1996).
- R. I. Barabash, *Mater. Sci. Eng. A* **309–310**, 49 (2001).
- T. Ungar, A. Revesz, A. Borbely, *J. Appl. Crystallogr.* **31**, 554 (1998).
- A. Hasnaoui, H. Van Swygenhoven, P. M. Derlet, *Acta Mater.* **50**, 3927 (2002).
- A. Hasnaoui, H. Van Swygenhoven, P. M. Derlet, *Phys. Rev. B* **66**, 184112 (2002).
- A. Hasnaoui, H. Van Swygenhoven, P. M. Derlet, *Science* **300**, 1550 (2003).
- Supported by Swiss National Science Foundation grant 21-65152.01. We thank A. Bollhalder and M. Schild for development of the in situ tensile machine, M. Victoria for fruitful discussions, and the team of the materials beamline of the SLS for technical support.

Supporting Online Material

www.sciencemag.org/cgi/content/full/304/5668/PAGE/DC1
Materials and Methods
Figs. S1 to S3
References

23 December 2003; accepted 11 February 2004

Many routes have been developed for the synthesis of carbon nanotubes, but their assembly into continuous fibers has been achieved only through post-processing methods. We spun fibers and ribbons of carbon nanotubes directly from the chemical vapor deposition (CVD) synthesis zone of a furnace using a liquid source of carbon and an iron nanocatalyst. This process was realized through the appropriate choice of reactants, control of the reaction conditions, and continuous withdrawal of the product with a rotating spindle used in various geometries. This direct spinning from a CVD reaction zone is extendable to other types of fiber and to the spin coating of rotating objects in general.

Macroscopic assemblies of carbon nanotubes are desired for a wide range of applications, including composites, micromechanical actuators, power cables, electrodes, and catalyst supports (1, 2). Considerable research has been directed toward producing assemblies of aligned nanotubes, with the object of obtaining good properties in one or more directions. To date, attention has focused on the postprocessing of dispersed nanotubes by drying to produce films (3–5), coupled with electric or magnetic fields (6–8). Similarly, fibers of nanotubes (9, 10) or nanotube-polymer blends (11–14) have been drawn or spun from solutions or gels. It has also been demonstrated that a thread of nanotubes can be dry-drawn from an aligned assembly on a silicon substrate (15), underlining the ability of nanotubes to assemble as a result of van der Waal interactions. Recently, Zhu *et al.* have reported the formation of a 20-cm-long nanotube thread after the pyrolysis of hexane, ferrocene, and thiophene (16–18). Although this work shows the possibility of fiber formation directly in a furnace, the product was isolated strands.

By mechanically drawing the carbon nanotubes directly from the gaseous reaction zone, we have found it possible to wind up continuous fiber without an apparent limit to the length. If this fiber can challenge conventional high-performance fibers for properties, its simpler method of production will commend it on both cost and environmental grounds. The key requirements for continuous spinning are the rapid production of high-purity nanotubes to form an aerogel (19) in the furnace hot zone and the forcible removal of the product from reaction by continuous wind-up. We selected ethanol as the carbon source, in which 0.23 to 2.3 weight percent (wt %) ferrocene and 1.0 to 4.0 wt % thiophene were dissolved. The solution was then

injected at 0.08 to 0.25 ml/min from the top of the furnace into a hydrogen carrier gas that flowed at 400 to 800 ml/min, with the furnace hot zone in the range of 1050° to 1200°C (Fig. 1).

Under these synthesis conditions, the nanotubes in the hot zone formed an aerogel, which appeared rather like “elastic smoke,” because there was sufficient association between the nanotubes to give some degree of mechanical integrity. The aerogel, viewed with a mirror placed at the bottom of the furnace, appeared very soon after the introduction of the precursors (Fig. 2). It was then stretched by the gas flow into the form of a sock, elongating downwards along the furnace axis. The sock did not attach to the furnace walls in the hot zone, which accordingly remained clean throughout the process.

When no attempt was made to draw the aerogel out of the furnace by mechanical means, it traveled down the furnace tube with the gas flow. The gas flow was stable in the lower half of the furnace because it decelerated with decreasing temperature as its density increased, which prevented convection. As the aerogel reached the cool end of the furnace tube (~500°C), it attached to the walls and formed a diaphanous membrane across the tube that thickened with time.

Convection currents occurred in the upper half of the furnace and were enhanced by the injection of comparatively cool feedstock down the axis. We believe that the gas moved upward adjacent to the furnace walls and downward in the center of the tube. As a consequence of this circulation, portions of the nanotube aerogel appeared to be carried upward, and then to stick to the cooler wall or injector to form a fiber that hung down the furnace axis. This fiber then continued to grow when additional nanotubes adhered to it. These fibers may be similar to those reported by Zhu *et al.*, although they play no part in the continuous process that we report here.

The aerogel could be continuously drawn from the hot zone by winding it onto a rotating rod. In this way, the material was concentrated near the furnace axis and kept clear of the cooler furnace walls, thus avoiding the forma-

Department of Materials Science and Metallurgy, University of Cambridge, Pembroke Street, Cambridge CB2 3QZ, UK.

*To whom correspondence should be addressed. E-mail: ahw1@cam.ac.uk

tion of a membrane. We evaluated several possible wind-up protocols with different geometries and spinning temperatures. In one of these protocols (Fig. 1A), the spindle was aligned at $\sim 25^\circ$ to the furnace axis and is rotated about that axis at 90 rpm. The device penetrated the hot zone to capture the aerogel before it reached the cool region (Fig. 2). When the area covered by this spindle was 12% of the cross section of the tube, the majority of the nanotubes produced could be captured and continuous spinning was achieved (movie S1). This spinning geometry produced continuous fibers with a degree of twist, which were collected either at the top of the spindle or along its length. Fibers were unwound from the spindle and wound up onto another rod (Fig. 3A).

In a second wind-up geometry (Fig. 1B), the spindle was rotated normal to the furnace axis outside the hot zone, at a position where the temperature was $\sim 100^\circ\text{C}$ (fig. S1). The advantage of this geometry is that well-defined, thin, unentangled films could be obtained when the wind-up speed was close to the velocity of the gas. When wind-up speed increased, the thin films separated into discrete threads that were wound simultaneously onto the spindle.

The composition of the spun materials, in terms of multiwalled nanotubes (MWNTs) or single-walled nanotubes (SWNTs), could be controlled by adjusting the reaction conditions. With ethanol feedstock, MWNTs formed with a thiophene concentration of 1.5 to 4.0 wt %, a hydrogen flow rate of 400 to 800 ml/min, and a synthesis temperature of 1100° to 1180°C ; SWNTs formed when the concentration of thiophene was reduced to ~ 0.5 wt % and the hydrogen flow rate was increased to ~ 1200 ml/min, at a synthesis temperature of up to 1200°C .

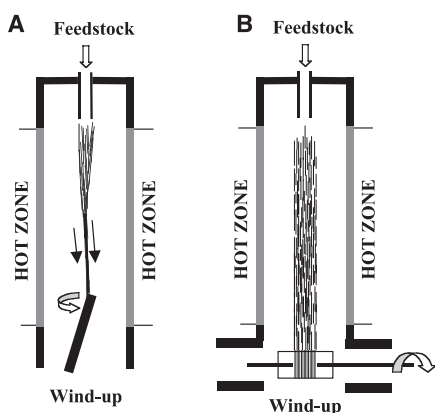


Fig. 1. (A) Schematic of the direct spinning process. The liquid feedstock, in which small quantities of ferrocene and thiophene are dissolved, is mixed with hydrogen and injected into the hot zone, where an aerogel of nanotubes forms. This aerogel is captured and wound out of the hot zone continuously as a fiber or film. Here, the wind-up is by an offset rotating spindle. (B) Schematic of the wind-up assembly that operates at a lower temperature, outside the furnace hot zone.

In order to achieve a clean product, it is important that the final stage in the reaction chain to produce carbon is finely balanced, so as to discourage the formation of nonfibrous particles with the nanotubes. Experimentally, a high hydrogen flow rate was found to suppress carbon formation, whereas the removal of hydrogen (and its replacement by argon) led to the precipitation of particulate carbon rather than nanotubes. The conditions in which SWNTs formed in preference to MWNTs required a considerably increased hydrogen flow rate and would thus appear to be those that are less susceptible to the formation of carbon. It is thought that the presence of oxygen as a component of the feedstock molecules, making possible the formation of carbon monoxide, reduces the tendency to deposit nonfibrous carbon in the absence of nucleating iron nanoparticles. The actual role played by thiophene in nanotube growth is still open to question; however, it is well known that sulfur plays a major role in promoting carbon-hydrocarbon reactions, especially when associated with iron. Its use in the vapor phase production of carbon fibers (20) is only one application, as the iron-sulfur combination is also used in the liquefaction of coal (21) and in other hydrogen/dehydrogenation reactions.

This continuous spinning process is possible with a range of carbon sources. Keeping all other conditions the same, we have replaced the ethanol with diethylether $[(\text{C}_2\text{H}_5)_2\text{O}]$, polyethylene glycol $[-(\text{CH}_2-\text{CH}_2-\text{O})_n]$, 1-propanol $(\text{CH}_3\text{CH}_2\text{CH}_2\text{OH})$, acetone $(\text{CH}_3\text{OCH}_3)$, and ethylformate $(\text{CH}_3\text{CH}_2\text{COOH})$: all oxygen-containing species, but with different oxygen groups. On the other hand, aromatic-hydrocarbons such as benzene (C_6H_6) , hexane $(\text{C}_6\text{H}_{14})$, and mesitylene $[\text{C}_6\text{H}_3(\text{CH}_3)_3]$ and mixed hydrocarbons such as petroleum led to the deposition of carbon particles, thick fibers, or both, but did not enable a sustained continuous spinning process unless they were mixed with another oxygen-containing molecule such as methanol.

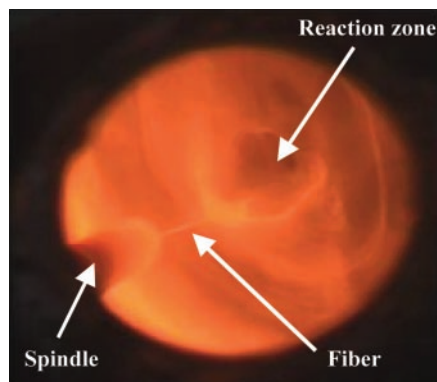


Fig. 2. A video frame view up the furnace, showing the nanotubes being drawn from the aerogel into the fiber on the spindle. The geometry of the spindle is that shown in Fig. 1A. A similar experiment is shown in movie S1.

The alignment, purity, and structure of the fibers obtained from the ethanol-based reactions were characterized by electron microscopy, including image analysis, Raman spectroscopy, and thermogravimetric analysis. In the MWNT fibers, the nanotube diameters were 30 nm, with an aspect ratio of ~ 1000 (Fig. 3). They contained 5 to 10 wt % iron but no extraneous carbon particles. The quality of alignment of the nanotubes was measured from transforms of scanning electron microscope (SEM) images (Fig. 3). The full width (at half maximum) of the inter-nanotube interference peak measured around the azimuthal circle was $\sim 11^\circ$ (fig. S2). However, there are indications that the degree of alignment can be improved if greater tension is applied to the fiber during processing. The SWNT fibers contained more impurities than the MWNT fibers, with the proportion of SWNTs estimated from transmission electron microscope observations as being >50 volume percent. The SWNTs had diameters between 1.6 and 3.5 nm and were organized in bundles with lateral dimensions of 30 nm. Raman spectra reveal the typical radial breathing modes, with peaks at 180, 243, and 262 cm^{-1} with a 514.5-nm excitation laser (fig. S3). The purity of

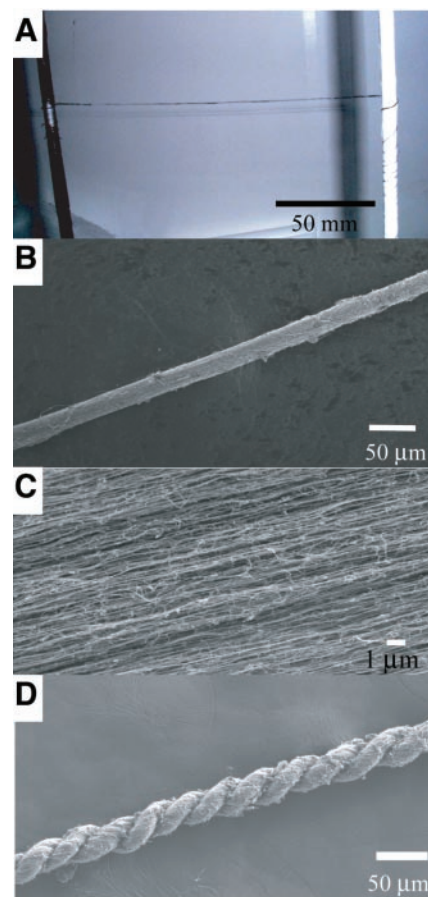
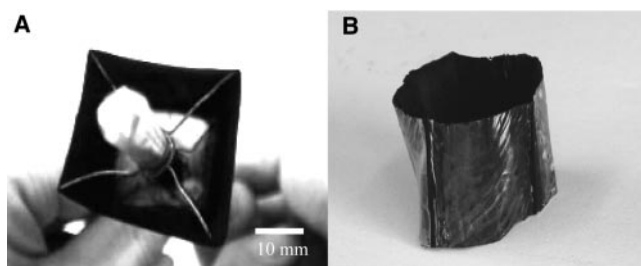


Fig. 3. (A) Photograph of nanotubes being wound from the spindle (left) onto a second spindle (right). (B and C) SEM micrographs of a fiber that consists of well-aligned MWNTs. (D) A permanent twist introduced into a nanotube fiber after its removal from the furnace.

Fig. 4. (A) An end view of nanotubes wound onto a square wire former to cover it. (B) A wound nanotube covering after infiltration with polyvinyl chloride and removal of the former.



MWNTs in fibers spun at high temperatures was higher (85 to 95 wt % purity) than for material collected from the furnace without spinning (70 to 85 wt % purity). In the latter case, it is possible that iron particles that did not generate nanotubes were effectively caught by the nanotube membrane that formed across the cold end of the furnace. Figure 3, B and C, shows SEM images of a fiber wound up with the offset rod. The alignment of the nanotubes along the fiber axis is apparent in the higher magnification image (Fig. 3C), whereas Fig. 3D shows the fiber's ability to hold a twist imparted after removal from the rod. The best electrical conductivity measured along a fiber was $8.3 \times 10^5 \Omega^{-1} \text{ m}^{-1}$, which is slightly higher than the typical value for carbon fibers (22). Preliminary mechanical measurements indicate that the fibers have a range of strengths, dependant on process conditions, between 0.05 N/Text and 0.5 N/Text (equivalent to 0.10 and 1.0 GPa, assuming a density of 2.0 g/cc, which is within the range of typical carbon fibers). The strain to failure was variable, but could exceed 100% on initial loading. There remains considerable potential to improve properties through process control and postprocess treatments.

Finally, in addition to its ability to spin nanotube fibers, the present process can be extended to the production of nonwoven, macroscopic objects by spin coating differently shaped formers. The alignment of the nanotubes and the thickness of the coatings can be reasonably controlled by the rotation speed and coating time. We demonstrated this process with a hollow frame, rotated normal to the furnace axis, that became covered with an aligned nanotube film (Fig. 4A). An extension of this process is to infiltrate the nanotube covering with a resin, to produce a composite shell from which the former can be removed (Fig. 4B).

This direct spinning process will allow one-step production of nanotube fibers, ribbons, and coatings with potentially excellent properties and wide-range applications. Furthermore, the success of this direct spinning process from the gas phase implies that similar processes could be applied to other fibrous materials that can be synthesized directly from the vapor phase.

References and Notes

- R. H. Baughman, A. A. Zakhidov, W. A. de Heer, *Science* **297**, 787 (2002).
- P. J. F. Harris, *Carbon Nanotubes and Related Structures* (Cambridge Univ. Press, Cambridge, 1999).
- M. S. P. Shaffer, X. Fan, A. H. Windle, *Carbon* **36**, 1603 (1998).
- T. V. Sreekumar *et al.*, *Chem. Mater.* **15**, 175 (2003).

- Y.-H. Li *et al.*, *Chem. Mater.* **14**, 483 (2002).
- B. W. Smith *et al.*, *Appl. Phys. Lett.* **77**, 663 (2000).
- J. E. Fischer *et al.*, *J. Appl. Phys.* **93**, 2157 (2003).
- M. J. Casavant, D. A. Walters, J. J. Schimdt, R. E. Smalley, *J. Appl. Phys.* **93**, 2153 (2003).
- V. A. Davis *et al.*, *Macromolecules* **37**, 154 (2004).
- H. H. Gommans *et al.*, *J. Appl. Phys.* **88**, 2509 (2000).
- B. Vigolo *et al.*, *Science* **290**, 1331 (2000).
- P. Poulin, B. Vigolo, P. Launois, *Carbon* **40**, 1741 (2002).
- B. Vigolo, P. Poulin, M. Lucas, P. Launois, P. Bernier, *Appl. Phys. Lett.* **81**, 1210 (2002).
- A. B. Dalton *et al.*, *Nature* **423**, 703 (2003).
- K. Jiang, Q. Li, S. Fan, *Nature* **419**, 801 (2002).
- H. Zhu *et al.*, *Science* **296**, 884 (2002).

- H. Zhu, B. Jiang, C. Xu, D. Wu, *Chem. Commun.* **2002**, 1858 (2002).
- B. Wei, R. Vajtai, Y. Y. Choi, P. M. Ajayan, *Nano Lett.* **2**, 1105 (2002).
- The nanotubes had a measure of coherence as an aerogel, and it is this property that aids spinning. However, there is no doubt that in the early stages of the synthesis, when a nanotube has only just started to grow from the metal particle and interaction between different nanotubes is weak, the phase would be more correctly described as an aerosol.
- A. Hoqu, M. K. Alam, G. G. Tibbetts, *Chem. Eng. Sci.* **56**, 4233 (2001).
- R. K. Sharma, J. S. MacFadden, A. H. Stiller, D. B. Dadyburjor, *Energy Fuels* **12**, 312 (1998).
- W. D. Callister Jr., *Materials Science and Engineering* (Wiley, New York, ed. 4, 1997), p. 798.
- We thank S. Cash, M. Jaffe, Q. Li, M. Motta, and P. Smith for their assistance. Supported by Thomas Swan and Co. Ltd.

Supporting Online Material

www.sciencemag.org/cgi/content/full/1094982/DC1
Figs. S1 to S3
Movie S1

22 December 2003; accepted 23 February 2004
Published online 11 March 2004;
10.1126/science.1094982
Include this information when citing this paper.

Reversible Optical Transcription of Supramolecular Chirality into Molecular Chirality

Jaap J. D. de Jong,¹ Linda N. Lucas,² Richard M. Kellogg,² Jan H. van Esch,^{1*} Ben L. Feringa^{1*}

In nature, key molecular processes such as communication, replication, and enzyme catalysis all rely on a delicate balance between molecular and supramolecular chirality. Here we report the design, synthesis, and operation of a reversible, photoresponsive, self-assembling molecular system in which molecular and supramolecular chirality communicate. It shows exceptional stereoselectivity upon aggregation of the molecules during gel formation with the solvent. This chirality is locked by photochemical switching, a process that is subsequently used to induce an inverted chiral supramolecular assembly as revealed by circular dichroism spectroscopy. The optical switching between different chiral aggregated states and the interplay of molecular and supramolecular chirality offer attractive new prospects for the development of molecular memory systems and smart functional materials.

The challenge of controlling chirality at different hierarchical levels (1–3) is particularly evident in the context of molecular self-assembly, protein folding, and the design of memory systems, sensors, and nanostructured materials (4–6). Chiral optical molecular switches offer fascinating opportunities, because molecular and supramolecular chirality might be tunable by light in a fully reversible manner. Elegant chiral optical switches, photoresponsive host-guest systems, and receptors have been reported (7). However, studies of self-assembling systems

(8–11) in which the macroscopic properties are affected by light have been limited to switchable organogels (12), receptors (13), and self-assembling peptide tubes (14, 15).

The molecular system presented here is based on a dithienylethene photochromic unit functionalized with (*R*)-1-phenylethylamine-derived amides (Fig. 1) (16). The self-assembly behavior of **1**, which arises from the formation of multiple hydrogen bonds between the amide groups, can be influenced by light. The dithienylethene **1** exists as two antiparallel, interconvertible open forms with *P*- and *M*-helicity, which cyclize in a fully reversible manner upon irradiation with ultraviolet (UV) light to two diastereoisomers of ring-closed product **2** (17). The light-induced switching between **1** and **2** is attended by changes in both the electronic properties and

¹Laboratory of Organic Chemistry, Stratingh Institute, University of Groningen, Nijenborgh 4, 9747 AG Groningen, Netherlands. ²Syncom, Kadijk 3, 9747 AT Groningen, Netherlands.

*To whom correspondence should be addressed. E-mail: esch@chem.rug.nl (J.H.E.); feringa@chem.rug.nl (B.L.F.)